

INTER-COMPARISON OF THEOS AND LANDSAT-5 TM OVER THE LIBYA 4 PSEUDO-INVARIANT CALIBRATION SITE

Morakot KAEWMANEE^{a*}, Larry LEIGH^a, Chaichat MUSANA^b and Panatda KIETLEADSEREE^b

^aImage Processing Lab, South Dakota State University
Daktronics Engineering Hall, Room 315
PO BOX 2222, SDSU, Brookings, SD 57007 USA;
Tel: +1(605) 688-4372; Fax: +1(605) 688-4969

^bGeo-Informatics and Space Technology Development Agency (Public organization),
120 (Building B) Chaeng Wattana Road, Laksi District, Bangkok 10210, Thailand;
Tel: +66(0) -2141-4470; Fax: +66(0) -2143-9586

E-mail: (morakot.kaewmanee, larry.leigh)@sdstate.edu
(chaichat.panatda)@eoc.gistda.or.th

KEY WORDS: Inter-comparison, sensors, THEOS, Landsat-5 TM, Libya 4, PICS, BRDF, SBAF, calibration

ABSTRACT: THEOS has been in orbit since October 2008 providing remotely sensed data to users for numerous applications to monitor global change over long periods of time with an imaging satellite requires a satellite system to exhibit a high degree of radiometric stability. Thus, it is critical to monitor the radiometric performance of these systems in order to accurately identify changes on the surface without confusing them with changes occurring due to the sensor. This paper presents a study trending the long term stability of THEOS based on work done to trend the Landsat 5 Thematic Mapper.

Landsat 5 and Landsat 7 are known to be well calibrated and trended over their lifetime. Recently, a promising new calibration approach has been introduced to perform radiometric calibration using sites around the globe which are stable over time and, thus, can provide a precise measure of sensor stability. An ideal site would be subject to minimal change over time such as arid land with high reflectance and sparse rainfall and vegetation. The site should also be located at high altitude in order to reduce atmospheric effects and exhibit minimal cloud cover. Pseudo-invariant calibration sites (PICS) have been developed for this purpose. For this study, the Libya 4 PICS was selected because Landsat 5 TM calibration trending using Libya 4 provides a precision well within 3%.

This study focuses on a series of THEOS and Landsat 5 TM images over Libya 4 taking advantage of the fully calibrated Landsat 5 TM. THEOS will be trended over its lifetime using Libya 4 and sensor degradation will be evaluated. In addition, due to the similarities between the relative spectral response of the two sensors, THEOS will be cross-calibrated to Landsat 5 TM to obtain an on-orbit absolute radiometric calibration over its entire lifetime.

1. INTRODUCTION

THEOS (Thailand Earth Observation Satellite) is Thailand's first remote sensing satellite which was manufactured by the French prime contractor-EADS Astrium and operated by THEOS engineers, team GISTDA (Geo-Informatics and Space Technology Development Agency). It was launched into sun-synchronous orbit on the 1st October, 2008. Recently, His Majesty the King of Thailand has renamed "THEOS" to "Thaichote" signifying the glory of Thailand (GISTDA, 2012). Thaichote has been providing remotely sensed data to users for many applications such as natural resources and environmental monitoring in the area of forestry management, agricultural change detection, coastal change monitoring, flood risk management and prevention etc.

The Landsat 5 TM satellite is selected for the inter-comparison with Thaichote because of a) the similarity of spectral bands in the visible and near infrared; b) it has been extensively and frequently used as a main inter-calibration sensors for radiometric calibration; c) it has been well calibrated throughout its lifetime and proven to be one of the most stable sensors (Hill et al, 1990 and Steven et al, 2003 and Helder et al, 2010); and d) the archived L5TM images could be used as a reference for many natural resources and environmental monitoring applications using Thaichote images.

Landsat 5 TM sensors have acquired images over the world for the past 27 years with its large swath width of 180 kilometers, a spatial resolution of 30 meters and 16days revisiting period. Thaichote has a spatial resolution of 15 meters and 90 kilometers swath width and 26 days revisiting time. The first four spectral bands, i.e. the visible and near infrared bands, for both Thaichote and L5 TM have similar spectral characteristics as seen in Table 1. L5 TM sensors gain calibration was updated in 2003 to remove the dependence on the changing IC (Internal Calibrator) lamps for band 1-5 and band 7, based on lifetime radiometric calibration curves derived from the detectors' responses IC (Integrated Circuit), inter-calibration with ETM+ and vicarious measurements. In 2007, the gains were further revised based on the detectors' responses to pseudo-invariant desert sites and inter-calibration with ETM+ (Chander et al, 2009).

Digital Number (DN) from one sensor has no relation to a DN from a different sensor. Thus, the conversion of DN to absolute radiance values is a necessary step for comparative analysis of spectral response of several images taken by different sensors.

Numerous on-orbit calibration studies have been done using pseudo invariant calibration sites (PICS) to monitor satellite calibration i.e. trending stability of a sensor and for the inter-comparison of one sensor to another. Helder et al (2010) has developed an algorithm to identify potential PICS for radiometric calibration trending of Landsat 5 TM using the CEOS (Committee on Earth Observation Satellite) reference sites which includes locations in Libya, Algeria and Mauritania (http://calval.cr.usgs.gov/sites_catalogu_ceos_sites.php#CEOS). The results from this work have shown that Lybia4 (location) has proven to be suitable for monitoring long-term trends in the visible and near-infrared wavelength regions with a variability of 2-3 % without compensation for atmospheric or surface effects. It is located at WRS-2 Path/Row (181/40), latitude °N [29.75;29.48;28.25;27.99] and longitude °E [23.13;24.86;22.75;24.48]. This study will compare Thaichote and Landsat 5 TM spectral radiance to monitor the sensors stability over Libya 4 -PICS.

The use of multitemporal data sets which use L5 TM for historical 1984-2011 and Thaichote for 2009 and beyond will provide invaluable information for monitoring environmental change both in Thailand and at a global scale. In order to combine images obtained from these two sensors, it is mandatory to identify the radiometric accuracy and a high degree of stability of the sensor with consideration of the reflective spectral response performance of sensors i.e. at sensor spectral radiance or Top-of-Atmosphere reflectance prior to the use of combined data. This paper presents a comparison of Thaichote and L5 TM at sensor spectral radiance reflectance and summarizes a study tracking the long term stability of Thaichote at- sensor spectral radiance based upon the methodology used to trend the Landsat 5 Thematic Mapper over Libya 4 Pseudo-Invariant Calibration Sites (PICS).

Table 1. Thaichote and L5 TM sensor characteristics of four spectral bands, data processing level, acquisition mean, geometric and radiometric quality used in the study.

	Thaichote	Landsat 5 TM	Remarks
Image Processing Level & Acquisition Source	Level 1A Thaichote Image Ground Segment System	L1T Generated from Landsat website	
Spectral Bands	Band range (nm)	Band range (nm)	
Band1 Blue	450-520	450-520	
Band2 Green	530-600	520-600	Landsat 5 TM
Band3 Red	620-690	630-690	Band5-7 are not
Band4 NIR	770-900	760-900	used in this study
Image Bands Ordering	Band3-Band2-Band1-Band4	Band1-Band2-Band3-Band4	
Spatial Resolution	15 m	30 m	
Image Swath Width	183 km	90 km	
Image acquisition dataset	June 2009-August, 2012	Jan 2008 – October 2011	

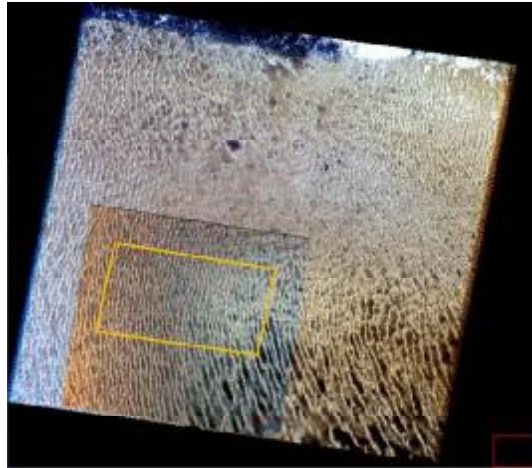


Figure 1. The Study Area, Landsat 5 TM and Thaichote over Libya4 Pseudo Invariant Calibration Site

2. METHODS AND EQUATIONS

Satellite Dataset

The imagery dataset used in this study consisted of seventy-one Thaichote and fifty-two Landsat 5 TM images over Libya 4 PICS. The collection of Thaichote images was from June 2009 to August 2012 with satellite view viewing angle around 15 degree. The L5 TM images were acquired from January 2008 to November 2011. The reason for having differences in time periods between these two sensors was, firstly, L5 TM has been well calibrated throughout its lifetime and proven to be one of the most stable sensors (Hill et al, 1990 and Steven et al, 2003 and Helder et al, 2010); thus, by selecting L5 TM over Libya-4 PICS 1 year before Thaichote was launched is adequate to demonstrate the stability of L5 TM sensor. Secondly, although Thaichote was launched on 1 October 2008, the commissioning phase was formally announced as successful in June 2009. Thirdly, L5 TM images were available up to October, 2011. Due to a rapidly degrading electronic component (downlinking capability), the U.S. Geological Survey (USGS) stopped acquiring L5 TM images on 18 November 2011. After several attempts to fix the problem, the L5 TM has ceased routine acquisition as of May 8, 2012 (USGS, 2012). Lastly, Thaichote is still acquiring data continually which will continue, at least, for its expected design lifetime of 5 years. Therefore, we select the last 3 years imagery dataset of each sensor to study the inter-comparison of sensor stability. The image processing level, sensor characteristics, image bands ordering and image dataset are listed in Table 1. L5 TM satellite view angles are generally near nadir, and the solar zenith angle ranges of Libya 4 PICS images used in the study were from 22° to 58°. Thaichote satellite view angles and the solar zenith angles ranges were from +/- 16° and from 15° to 58°, respectively.

The Study Area

The study area is a section of the Libya 4 PICS site, latitude °N [28.44;28.72;28.37;28.47] and longitude °E [23.11;23.85;23.76;23.02], with approximately 73 x 40 kilometers as seen in Figure 1. The chosen area size represents the largest union area of all Thaichote and L5 TM images in this study.

Satellite data Processing

The image dataset for both Thaichote and Landsat 5 TM were Level 1A and L1T products which are corrected radiometrically. Thaichote images were processed by Thaichote Image Ground Segment System. L5 TM images were downloaded from the USGS Global Visualization Viewer (<http://glovis.usgs.gov>). The images were georeferenced using the headerfiles. The study area of 73 x 40 km is extracted from the image by subsetting the image band by band and

storing for further at-sensor spectral radiance conversion. Even though, a visual inspection was done to primarily select cloud-free images, saturated pixels (DN = 254) and dark pixels (DN=0) were masked out during the image subsetting process.

At-sensor Spectral Radiance Conversion

At-sensor spectral radiance is calculated by converting digital number(DN) using the sensor gains. The sensor gains can be obtained from Thaichote and L5 TM headerfiles. Thaichote at-sensor spectral radiance conversion for each band can be calculated using the following equation.

$$L_{\lambda}^{iThaichote} = \frac{DN_i}{Gain_i} \quad (1)$$

Where $L_{\lambda}^{iThaichote}$ is the at-sensor spectral radiance of Thaichote for band i ($Wm^{-2}.sr^{-1}.\mu m^{-1}$);

DN_i is the digital number of band i ;

$Gain_i$ is the Thaichote gain for band i ;

Landsat 5 TM at-sensor spectral radiance conversion for each band can be calculated using the following equation (Chander et al, 2009).

$$L_{\lambda}^{iLS5TM} = \left[\frac{(L_{Max\lambda}^i - L_{Min\lambda}^i)}{(DN_{Max}^i - DN_{Min}^i)} \right] * (DN^i - DN_{Min}^i) + L_{Min\lambda}^i \quad (2)$$

Where L_{λ}^{iLS5TM} is at-sensor spectral radiance of Landsat 5 TM for band i ($Wm^{-2}.sr^{-1}.\mu m^{-1}$);

DN^i is the digital number of band i ;

DN_{Max}^i and DN_{Min}^i are the maximum (255) and minimum (1) digital number for band i ;

$L_{Max\lambda}^i$ and $L_{Min\lambda}^i$ are at-sensor spectral radiance scaled to DN_{Max}^i and DN_{Min}^i for band i ;

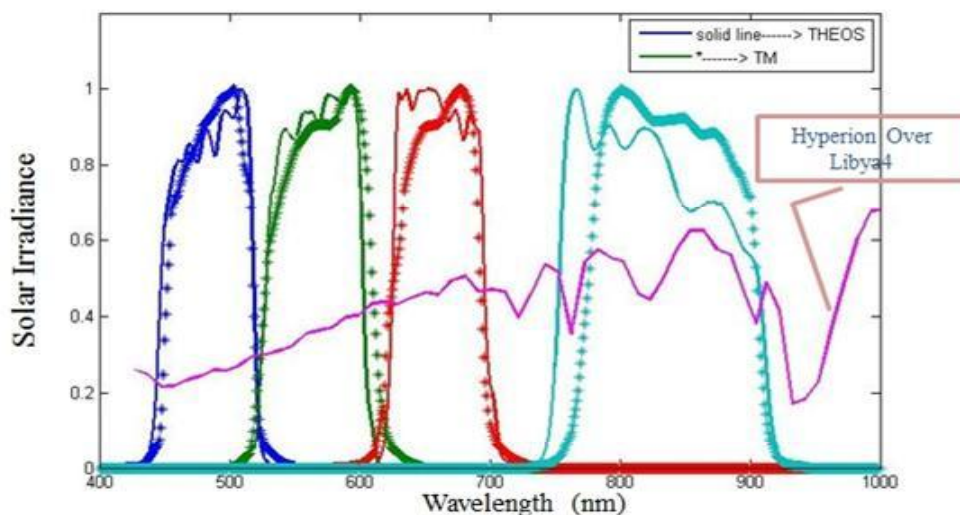


Figure 2. The L5 TM and Thaichote relative spectral response and Hyperion spectral profile over Libya-4
 Source: Geo-Informatics and Space Technology Development Agency (Public Organization) ; CEOS.

At-sensor Spectral Radiance Normalization

At sensor spectral radiance correction is calculated by applying an Earth-Sun distance and Sun angle correction to each band of the image to remove the cosine effect of different solar zenith angles due to the time difference during image acquisitions and correct for the variation in the Earth-Sun distance between different image acquisition dates. These variations can be significant depending on geographical location and acquisition time. Figure-3 shows the L5 TM and Thaichote at-sensor spectral radiance comparison before and after correction for solar zenith angles and time variation. Each image pixel was multiplied by the square of the ratio of the actual Earth-Sun distance in astronomical unit (au) to 1 au to perform the Earth-Sun distance correction. The sun angle effect was normalized to a nadir viewing geometry for all L5 TM scenes by dividing the spectral radiance value of each image pixel by the cosine of the solar zenith angle. L5 TM satellite view angles are normally near nadir therefore there is no need to apply satellite view angles correction as seen in Equation (4).

Thaichote satellite is an agile satellite, it can be maneuvered to acquire an image with a pitch and roll angles of up to +/- 30 degrees. The satellite view angle can be obtained by taking into account the square root of the sum of the square of pitch and roll angles. Therefore to get Thaichote and L5 TM on the same basis it is required that the Thaichote at-sensor spectral radiance to be corrected for satellite view angles as in Equation (5).

The equation for calculating a standard Earth-Sun distance (Van Leeuwen, 2012), for sun angle correction, and for satellite view angle correction are listed below:-

$$d = 1 + 0.01672 * \sin\left(\frac{2 * \pi * (JD - 93.5)}{365}\right) \quad (3)$$

Where d is a standard Earth-Sun distance ; JD is the Julian day number.

$$L_{\lambda TM, corrected}^i = \frac{d^2 * L_{\lambda LS5TM}^i}{\cos \theta_{sun}} \quad (4)$$

Where $L_{\lambda TM, corrected}^i$ is Landsat 5 TM at-sensor spectral radiance after the sun angle correction for band i ;

$L_{\lambda LS5TM}^i$ is Landsat 5 TM at-sensor spectral radiance for band i ; θ_{sun} is Landsat 5 TM Solar zenith angle;

$$L_{\lambda TH, corrected}^i = \frac{d^2 * L_{\lambda TH}^i}{\cos \theta_{sun} * \cos \theta_{sat}} \quad (5)$$

Where $L_{\lambda TH, corrected}^i$ is Thaichote at-sensor spectral radiance after sun and satellite view angle correction for band i ;

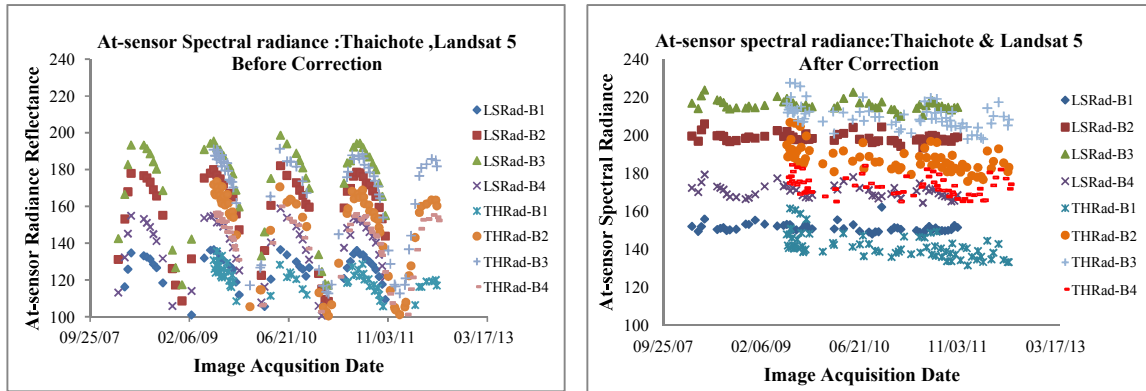
$L_{\lambda TH}^i$ is Thaichote at-sensor spectral radiance for band i ;

θ_{sun} is Thaichote solar zenith angle;

θ_{sat} is Thaichote satellite view angle.

Landsat 5 TM and Thaichote Relative Spectral Response Comparison

The sensor characteristics for both Thaichote and L5 TM are very similar in terms of spectral resolution; however, the Relative Spectral Response (RSR) are slightly different. This could result in an apparent spectral radiance difference when observing the same target. This difference RSR in the spectral bands between the two sensors can be compensated by taking into account the spectral profile of the target and the of the two sensors, which is referred to as a SBAF (Spectral Band Adjustment Factor) (Teillet et al , 2007, Chander, 2012). The L5 TM and Thaichote RSR and Hyperion spectral profile over Libya 4 is shown in Figure-2. Hyperion is an experimental hyperspectral satellite based sensors which is one of three sensors on board the EO-1 platform. The instrument is capable of providing 220 spectral bands from 0.4 to 2.5 microns with a 30 meters spectral resolution.



a)b)

Figure 3. Comparison Landsat 5 TM and Thaichote at-sensor spectral radiance. a) before and b) after correction of cosine of solar zenith and satellite view angle and time variation (Earth-Sun distance).

SBAF Calculation

The simulated spectral radiance for any sensor can be calculated by integrating the spectral response of the sensor with the hyperspectral spectral radiance profile at each sampled wavelength, weighted by the respective RSR as seen in equation (6). The integral in the numerator calculates the amount of in-band reflectance acquired in the respective RSR band and is divided by the integral of the RSR of the sensor so there is no net gain/loss due to the filter response function (Chander, 2012). The SBAF is calculated by integrating the spectral response of the L5 TM and Thaichote sensor with the hyperspectral spectral radiance profile at each sampled wavelength, weighted by the respective RSR as mentioned above, see equation (7). Thus SBAF, which is the ratio of simulated spectral radiance of L5 TM and Thaichote, gives a quantitative estimate of the difference between the observed reflectance of the two sensors arising from mismatch in the RSR for a given band and target as in equation (8). Table 2 displays the value of Thaichote SBAF over Libya 4-PICS.

$$\bar{L}_{\lambda}(\text{sensor}) = \frac{\int L_{\lambda} RSR_{\lambda} d\lambda}{\int RSR_{\lambda} d\lambda} \quad (6)$$

$$SBAF = \frac{\bar{L}_{\lambda(TM)}}{\bar{L}_{\lambda(TH)}} = \frac{(\int L_{\lambda} RSR_{\lambda(TM)} d\lambda) / (\int RSR_{\lambda(TM)} d\lambda)}{(\int L_{\lambda} RSR_{\lambda(TH)} d\lambda) / (\int RSR_{\lambda(TH)} d\lambda)} \quad (7)$$

$$\bar{L}_{\lambda(TH)}^* = \bar{L}_{\lambda(TH)} * SBAF \quad (8)$$

Where RSR_{λ} is Relative Spectral Response of the sensor [$(Wm^{-2}.sr^{-1}.\mu m^{-1})$];

L_{λ} is Hyperspectral spectral radiance profile generated from the EO-1 Hyperion [$(Wm^{-2}.sr^{-1}.\mu m^{-1})$];

$\bar{L}_{\lambda(TM)}$ is Simulated TM+ spectral radiance [$(Wm^{-2}.sr^{-1}.\mu m^{-1})$];

$\bar{L}_{\lambda(TH)}$ is Simulated Thaichote spectral radiance [$(Wm^{-2}.sr^{-1}.\mu m^{-1})$];

$\bar{L}_{\lambda(TH)}^*$ is Adjusted Thaichote spectral radiance using the SBAF to match the Landsat 5 TM [unitless];

First Order Bidirectional Reflectance Distribution Function (BRDF) Correction

The BRDF effect is due to the non-lambertian desert surface the effects of which can be seen by changes in the illumination geometry, by the variations in solar zenith and viewing angles. This study aims to develop a first order BRDF correction with respect to the solar zenith angles and satellite viewing angles for Thaichote and L5 TM time series dataset. The trend of the illumination effect can be seen by plotting spectral radiance of each sensor for each band with respect to solar zenith angles and satellite view angles. Then, the fitted linear regression models are calculated to identify the relationship between the spectral radiance and solar zenith and satellite viewing angle which is called the BRDF-Solar Zenith Model (BRDF-SZ) and BRDF-Viewing Angle Model (BRDF-VA) as seen in Equation (9) and

(11), respectively. The slope and intercept derived from these BRDF models are used to perform BRDF corrections. The BRDF-SZ correction is applied to SBAF corrected spectral radiance taking into account the slope and intercept of the BRDF-SZ model as seen in equation (10). Then, the BRDF-VA correction is applied to BRDS-SZ corrected spectral radiance, again taking into account the slope and intercept of the BRDF-VA model, as seen in equation (12). L5 TM satellite viewing angles are near nadir, therefore there is no need to apply BRDF-VA correction whereas the Thaichote spectral radiance must be corrected for both.

$$BRDF_{SZ}^i = a_0^i x + a_1^i \quad (9)$$

$$Corr.BRDF_{SZ} = Corr.SBAF_i * \left(a_1^i / (SZ_j * a_0^i + a_1^i) \right) \quad (10)$$

$$BRDF_{VA}^i = b_0^i x + b_1^i \quad (11)$$

$$Corr.BRDF_{VA} = Corr.BRDF_{SZ} * \left(b_1^i / (VA_j * b_0^i + b_1^i) \right) \quad (12)$$

Where $BRDF_{SZ}^i, BRDF_{VA}^i$ are BRDF-SZ and BRDF-VA model for band i ;

a_0^i, b_0^i are the slope of BRDF-SZ and BRDF-VA model for band i ;

a_1^i, b_1^i are the intercept of BRDF-SZ and BRDF-VA model for band i ;

$Corr.SBAF_i$ is at sensor radiance after SBAF correction for each band i ;

$Corr.BRDF_{SZ}, Corr.BRDF_{VA}$ are at sensor radiance after BRDF-SZ and BRDF-VA correction ;

SZ_j, VA_j are solar zenith angle and satellite viewing angle for image j ;

3. RESULTS AND DISCUSSION

Comparison of measured corrected (or normalized) spectral radiance trends between Thaichote and Landsat 5 TM

The temporal stability of Thaichote and L5 TM over Libya4-PICS has been investigated for the four spectral bands in the visible and near infrared regions of the EM spectrum. The viewing geometry for L5 TM is nearly at nadir with Thaichote being pointable to within +/-16 degrees. Figure 3-a, shows the temporal trend of Thaichote and L5 TM at-sensor spectral radiance time series over Libya 4-PICS. 365 day annual cycles can be clearly seen which result from the combination of the solar zenith angles, time variation and BRDF effects. Figure 3-b, shows the trending after removing the Earth-Sun Distance, solar zenith and satellite view angle effects. The temporal uncertainty is calculated by finding the standard deviation and dividing by the mean. It was found that L5 TM and Thaichote temporal uncertainty was within 14% and 15.6% for each band, respectively before the correction as seen in Table 3. The change in spectral radiance with large solar zenith angles is seen in Figure 4-a, while in combination large satellite view angles contribute significantly to increasing apparent spectral radiance, as shown in Figure 4-b. A simple first order linear regression BRDF model was developed to correct for the variations which are dependent on the solar zenith and viewing angle of the acquisitions. Table 4 shows the first order BRDF-SZ and BRDF-VA model coefficients for Thaichote and L5 TM. After correction for these variations, temporal uncertainty is greatly reduced to produce a BRDF corrected net radiance uncertainty that is within 2% and 4% for L5 TM and Thaichote, respectively, as seen in Figure 4-c and Table 3.

Table 2. SBAF and Absolute Gain Scale Factor values to adjust Thaichote spectral radiance to match the Landsat 5 TM spectral radiance.

	Band 1	Band 2	Band 3	Band 4
SBAF	1.0068	1.0135	1.0028	1.0024
Absolute Gain Scale Factor	1.0427	1.0252	1.0043	0.9519

Thaichote Absolute Gain Scale Factor

Figure 4-c shows the spectral radiance comparison between L5 TM and Thaichote after applying the BRDF corrections. In order to identify the relationship of absolute radiance difference between these two sensors, the Absolute Gain Scale Factor (AGSF) is determined by averaging the spectral radiance of Landsat 5 TM divided by the mean of Thaichote spectral radiance for each band. Figure 4-d displays Thaichote's spectral radiance corrected by the AGSF to match L5 TM's spectral radiance. It can be clearly seen that both sensors are closely related in terms of absolute radiance because the absolute gain scale factor for all four bands is very close to 1, as shown in Table 2. The AGSF difference in bands 1 and 4, the blue and near infrared band, approach a 5% uncertainty; however, it is well within a comfort zone which could be a result of differences in RSR and a contribution of atmospheric effect i.e. aerosol in band 1 and water absorption in band 4 as verified in Figure 2.

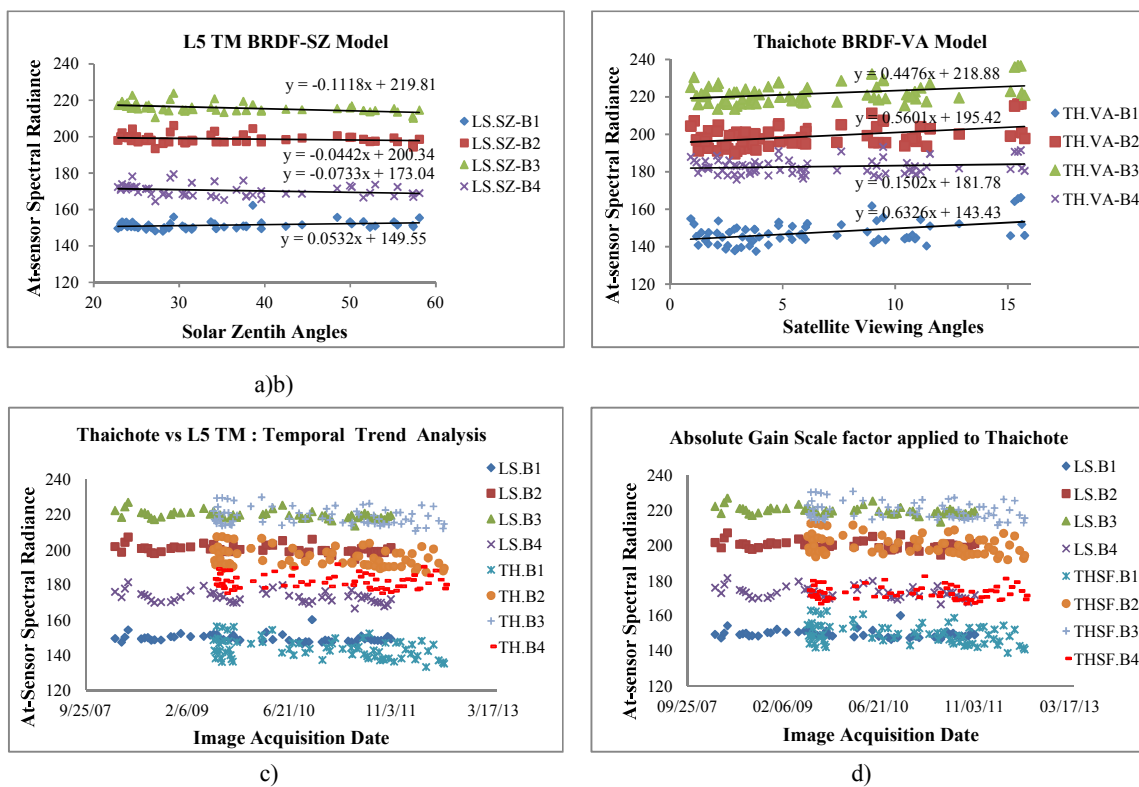


Figure 4. a) L5 TM BRDF-SZ Model b) Thaichote BRDF-VA Model c) Thaichote and L5 TM Temporal trend d) Thaichote after applying AGSF , L5 TM Temporal spectral radiance trend stability over Libya-4.

Table 3. The temporal trend stability before and after SBAF, BRDF corrections for Thaichote and L5 TM over Libya 4.

Thaichote	Band 1	Band 2	Band 3	Band 4	LS 5 TM	Band 1	Band 2	Band 3	Band 4
RAD.Mea	15.04%	15.36%	15.54%	15.16%	RAD.Mea	13.16%	13.67%	13.93%	13.96%
Corr. SBAF SZ-VA.	4.47%	3.46%	3.07%	2.91%	Corr. SZ	1.52%	1.19%	1.22%	1.94%
BRDF-SZ	4.16%	2.92%	2.35%	2.20%	BRDF-SZ	1.47%	1.16%	1.07%	1.88%
BRDF-VA	3.84%	2.70%	2.21%	2.19%					

Table 4. The first order BRDF-SZ and BRDF-VA model coefficients for Thaichote and Landsat 5 TM.

Thaichote BRDF Model		Band 1	Band 2	Band 3	Band 4	LS 5 TM BRDF Model		Band 1	Band 2	Band 3	Band 4
SZ	a_0	-0.141	-0.257	-0.319	-0.256	SZ	a_0	0.053	-0.044	-0.112	-0.073
	a_1	147.4	199.0	221.7	182.7		a_1	149.5	200.3	219.8	173.0
VA	b_0	0.633	0.560	0.448	0.150						
	b_1	143.4	195.4	218.9	181.8						

Table 5. Linear regression parameters of Thaichote and L5 TM temporal trend over Libya 4 and results of hypothesis test on slope of temporal series.

Thaichote		Band 1	Band 2	Band 3	Band 4	LS 5 TM		Band 1	Band 2	Band 3	Band 4
Temporal Trend	a_0	-0.0053	-0.0043	-0.0032	-0.0003	Temporal Trend	a_0	-0.0012	-0.0019	-0.0024	-0.0026
	a_1	147.5	198.7	221.4	182.0		a_1	160.58	218.53	242.66	197.48
%Degradation rate per year		-1.32%	-0.79%	-0.53%	-0.06%						
p-value		0.4195	0.3701	0.3420	0.8051						
Hypothesis Test		Fail to Reject	Fail to Reject	Fail to Reject	Fail to Reject						

Statistics Test for Thaichote Temporal trend

Landsat 5 TM and Thaichote temporal stability can be further studied when the BRDF correctioned data using equation (10) and (12) is for each of the sensors. Table 5 displays the best fit linear regression model coefficients for Thaichote and Landsat 5 TM. Figure 4-d illustrates the relationship of Thaichote BRDF corrected spectral radiance as plotted against days since launch.

It was found thatThachote sensor degradation rate per year is no greater than -1.4%, -0.8% , -0.6% and -0.1% for band 1,2,3 and 4 respectively, as seen in Table 5. In order to confirm whether Thaichote sensor is stable for the life of the instrument, a hypothesis test using a Student's t-test was performed on the slope to evaluate if the slope is statistically equal to zero. The null hypothesis states that slope equals zero, which corresponds to no drift in the absolute calibration of Thaichote. Whereas the alternative hypothesis states that the slope is statistically significant, then there is a drift in the absolute calibration. The results of hypothesis test confirmed that Thaichote sensor is stable for the entire operational life time in orbit,as seen in Table 5.

4. CONCLUSIONS AND RECOMMENDATIONS

The Libya 4 PICS was used to monitor the long term on orbit trend for L5 TM and Thaichote spectral radiance during 2008-2011 and 2009 to 2012, respectively. The use of the time series data reduced the impact of oscillation of spectral radiance due to solar zenith angles and satellite view angles and time variation. In order to account for the radiance variation attributable to viewing and illumination geometry, the measured spectral radiance have been corrected with a linear BRDF model. Prior to comparison of the in band radiances, Thaichote spectral radiance was adjusted by applying a SBAF to compensate for the difference in relative spectral response with respect to L5 TM. The spectral radiance temporal trend shows the variation caused by annual cycle oscillation is greatly reduced and the temporal stability is shown to be within 2% and between 2-4% for L5 TM and Thaichote, respectively.

It can be concluded that Thaichote sensor is very similar to LS 5 TM in terms of spectral response characteristics as confirmed by SBAF and AGSF values being close to 1. The Thaichote sensor is very stable as evaluated by a statistic t-test showing that there is no significant drift in all four bands over its nearly 4 years in orbit. In order to put Thaichote and L5 TM products on the same basis, it is recommended that an update to on-orbit absolute radiometric calibration parameters in Thaichote image processing system be performed or that imagery using the old absolute calibration parameters be corrected using the AGSF.

ACKNOWLEDGEMENTS

The authors thank the SDSU Image Processing Lab members for providing technical support, statistical data and helpful comments in this research. The gratitude is also extended to GISTDA and the Thaichote calibration/validation team for the support of Thaichote imageries and for supplying technical data.

REFERENCES:

References from Journals:

Angal, A., Xiong X., Choi, T., Chander, G., and Wu A., 2010, Using the Sonoran and Libyan Desert test sites to monitor the temporal stability of reflective solar bands for Landsat 7 enhanced thematic mapper plus and Terra moderate resolution imaging spectrometer sensors. *Journal of Applied Remote Sensing*, Vol.4, 043525.

Chander, G., Markham, B.L., Helder, D.L., 2009, Summary of current radiometric calibration coefficients for Landsat MSS, TM, ETM+, and EO-1 ALI sensors. *Remote Sens. Environ.* Vol.113, pp. 893-903.

Helder, D.L., Basnet, B., and Morstad, D.L., 2010. Optimized identification of worldwide radiometric pseudo-invariant calibration sites, *Canadian Journal of Remote Sensing*, Vol. 36, No.5, pp.57-539.

Hill, J., Aifadopoulou, D. 1990, Comparative analysis of Landsat-5 TM and SPOT HRV-1 data for use in multiple sensor approaches, *Remote Sens. Environ.* Vol.34, pp. 55-70.

Steven, D.M., Mathaus, J.T., Baret, F., Xu, H., Chopping, J.M., 2003, Intercalibration of vegetation indices from different sensor systems. *Remote Sens. Environ.* Vol.88, pp. 412-422.

Teillet, P.M., Fedosejevs, G., Thome, K.J., Barker, J.L., 2007, Impacts of spectral band difference effects on radiometric cross-calibration between satellite sensors in the solar-reflective spectral domain, *Remote Sensing of Environment* doi:10.1016/j.rse.2007.03.003

References from Other Literature:

CEOS, 2012. Committee on Earth Observation Systems, Spectral Response Function Information: Landsat-5 TM. Available online : <http://calvalportal.ceos.org/cvp/web/guest/landsat-5-tm> (accessed on 5 June 2012).

Chander, G., 2012, Radiometric Cross-calibration of EO-1 ALI with L7 ETM+ and Terra MODIS Sensors, Available online : http://calval.cr.usgs.gov/wordpress/wp-content/uploads/Chander_2012_04_ALI_v2VISID.pdf (accessed on 29 July 2012).

GISTDA, 2012, Geo-Informatics and Space Technology Development Agency (Public Organization), Ministry of Science and Technology, Bangkok, Thailand. Available online : <http://gistda.or.th> (accessed on 25 July 2012).

USGS, 2012, Landsat and LDCM Headlines Available online : http://landsat.usgs.gov/mission_headlines2011.php, http://landsat.usgs.gov/mission_headlines2012.php (accessed on 14 July 2012).

Van Leeuwen, 2012, University of Szeged, Department of Physical Geography and geoinformatics, Szeged, Hungary Available online: <http://www.geo.u-szeged.hu/~boud/teaching/preprocessing%20of%20satellite%20data.htm> (accessed on 24 May 2012).